© 2020 Chinese Physical Society and IOP Publishing Ltd Printed in China and the UK

Commun. Theor. Phys. **72** (2020) 045202 (7pp) https://doi.org/10.1088/1572-9494/ab6913

Role of the $\Lambda(1600)$ in the $K^- p \to \Lambda\pi^0\pi^0$ reaction

He Zhou[1,2] **and Ju-Jun Xie**[1,2,3]

[1] Institute of Modern Physics, Chinese Academy of Sciences, Lanzhou 730000, China
[2] School of Nuclear Science and Technology, University of Chinese Academy of Sciences, Beijing 101408, China
[3] School of Physics and Microelectronics, Zhengzhou University, Zhengzhou, Henan 450001, China

E-mail: xiejujun@impcas.ac.cn

Received 19 November 2019, revised 10 December 2019
Accepted for publication 17 December 2019
Published 30 March 2020

Abstract

Role of the $\Lambda(1600)$ is studied in the $K^- p \to \Lambda\pi^0\pi^0$ reaction by using the effective Lagrangian approach near the threshold. We perform a calculation for the total and differential cross sections by considering the contributions from the $\Lambda(1600)$ and $\Lambda(1670)$ intermediate resonances decaying into $\pi^0\Sigma^{*0}(1385)$ with $\Sigma^{*0}(1385)$ decaying into $\pi^0\Lambda$. Additionally, the non-resonance process from u-channel nucleon pole is also taken into account. With our model parameters, the current experimental data on the total cross sections of the $K^- p \to \Lambda\pi^0\pi^0$ reaction can be well reproduced. It is shown that we really need the contribution from the $\Lambda(1600)$ with spin-parity $J^P = 1/2^+$, and that these measurements can be used to determine some of the properties of the $\Lambda(1600)$ resonance. Furthermore, we also plot the $\pi^0\Lambda$ invariant mass distributions which could be tested by the future experimental measurements.

Keywords: $\bar{K}N$ scattering, effective Lagrangian approach, hyperon resonance

(Some figures may appear in colour only in the online journal)

1. Introduction

The $\bar{K}N$ scattering has been widely used to study the properties of the hyperon resonances [1–9], and it is extremely important to investigate these low excited hyperon states through the proposed K_L beam experiments at Jefferson Lab [10, 11]. By using a chiral unitary approach [12–15], the meson-baryon interactions are investigated and it was found that there are two poles in the neighbourhood of the well established $\Lambda(1405)$ state, which is actually a superposition of these two $J^P = 1/2^-$ resonances. Recently, within a dynamical coupled-channels model [16, 17], some hyperon resonance parameters are extracted through a comprehensive partial-wave analysis of the $K^- p \to \bar{K}N$, $\pi\Sigma$, $\pi\Lambda$, $\eta\Lambda$, and $K\Xi$ data up to invariant mass $W = 2.1$ GeV. Among the extracted resonances, a new narrow Λ^* resonance with $J^P = 3/2^+$ is also predicted in [16, 17]. On the contrary, Liu and Xie [18–20] analyzed the $K^- p \to \eta\Lambda$ reaction [21] with an effective Lagrangian approach and implied a new Λ^* resonance with $J^P = 3/2^-$. Its mass is about 1670 MeV, but its width is much smaller compared to one of the well established $\Lambda(1690)$ resonances. Thus, there are still some ambiguities of the Λ excited states that need to be clarified.

On the experimental side, the Crystal Ball Collaboration reported measurements with high precision of the $K^- p \to \Lambda\pi^0\pi^0$ reaction at eight incidents of K^- momenta between 514 and 750 MeV, corresponding to center of mass (c.m.) energies from 1569 to 1676 MeV [22]. It is shown that this reaction is dominated by the $\pi^0\Sigma^{*0}(1385)$ intermediate state in s-channel, and the contribution of the $f_0(500)$ meson in t-channel to the $K^- p \to \Lambda\pi^0\pi^0$ reaction appears to be very small and can be neglected. Indeed, it is shown that the contribution of scalar meson $f_0(500)$ and $f_0(980)$ from the $K^+K^- \to \pi^0\pi^0$ transition term is negligible [23, 24]. In addition, the strength of the total cross section of $K^- p \to \Lambda\pi^0\pi^0$ reaction could be well reproduced in terms of the large coupling of $\Lambda(1520)$ to $\pi\Sigma^*(1385)$, which is a prediction of the chiral unitary approach [24, 25]. On the other hand, with the aim of searching for the evidence for the possible Σ excited state with $J^P = 1/2^-$, which was predicted within the unquenched penta-quark models [26, 27], the $K^- p \to \Lambda\pi^+\pi^-$ reaction was investigated at the energy region of $\Lambda(1520)$ resonance peak by using the effective Lagrangian approach [28], where it is found that there is evidence for the existence of the new Σ^* state in the $K^- p \to \Lambda\pi^+\pi^-$ reaction.

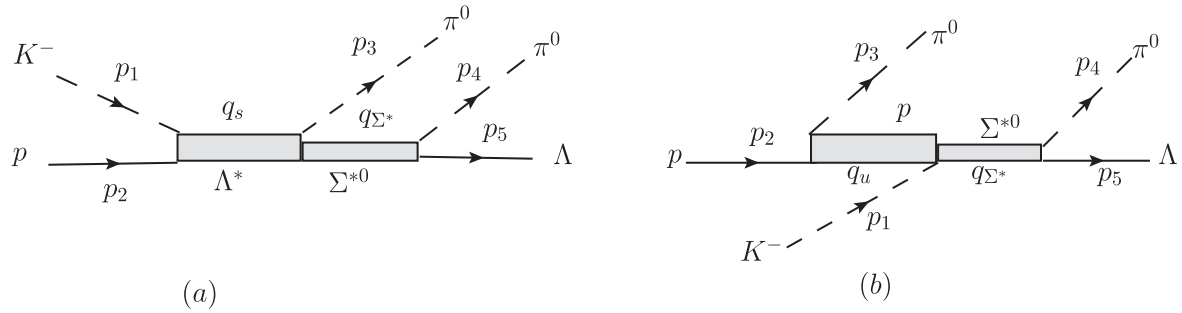

Figure 1. Feynman diagrams of the $K^-p \to \pi^0\pi^0\Lambda$ reaction. The contributions from s-channel $\Lambda(1600)$ and $\Lambda(1670)$ resonances and u-channel nucleon pole are considered. We also show the definition of the kinematical $(p_1, p_2, p_3, p_4, p_5)$ variables that we use in the present calculation. In addition, we use $q_s = p_1 + p_2$, $q_u = p_2 - p_3$, and $q_{\Sigma^*} = p_4 + p_5$.

For the $K^-p \to \Lambda\pi^0\pi^0$ reaction, the main contribution is from the Λ^* resonance through the process $K^-p \to \Lambda^* \to \pi^0\Sigma^{*0}(1385) \to \pi^0\pi^0\Lambda$. This reaction gives us a rather clean platform to study the isospin-0 Λ^* resonances because there are no isospin-1 Σ^* resonances that contribute to $K^-p \to \pi^0\Sigma^{*0}(1385)$. In the energy region of the current experimental measurements by the Crystal Ball Collaboration [22], there are two well established Λ^* resonances that give significant contributions: the three-star $\Lambda(1600)$ with $J^P = 1/2^+$ and the four-star $\Lambda(1670)$ with $J^P = 1/2^-$. Their Breit-Wigner masses and widths are [29]:

$$M_{\Lambda_1^*} = 1560 \sim 1700, \quad \Gamma_{\Lambda_1^*} = 50 \sim 250, \tag{1}$$

$$M_{\Lambda_2^*} = 1660 \sim 1680, \quad \Gamma_{\Lambda_2^*} = 25 \sim 50, \tag{2}$$

all in units of MeV and for which we have used the notation Λ_1^* and Λ_2^* to refer to the $\Lambda(1600)$ and $\Lambda(1670)$ resonances, respectively. It is interesting to notice that both the mass and width of the $\Lambda(1600)$ resonance have large uncertainties, while the ones for $\Lambda(1670)$ resonance are much more precise. Furthermore, in the work of [7], the most precise data on the $K^-p \to \pi^0\Sigma^0$ reaction were analyzed in the study of Λ^* resonances, and it is found that the $\Lambda(1600)$ resonance is definitely needed. The fitted resonance parameters for the $\Lambda(1600)$ are $M_{\Lambda(1600)} = 1574.7 \pm 0.5$ MeV and $\Gamma_{\Lambda(1600)} = 81.9 \pm 1.1$ MeV [7]. So, we expect that the $\Lambda(1600)$ resonance may also have a significant contribution to the $K^-p \to \Lambda\pi^0\pi^0$ reaction. In fact, the energy dependence of the total cross section of $K^-p \to \Lambda\pi^0\pi^0$ reaction [22] has a broad shoulder around the energy region of the $\Lambda(1600)$ state.

In the present work, based on the experimental measurements of the Crystal Ball Collaboration [22], we study the role of the $\Lambda(1600)$ and $\Lambda(1670)$ resonances in the $K^-p \to \Lambda\pi^0\pi^0$ reaction within the effective Lagrangian method and the resonance model. In addition, the non-resonance process from the u-channel nucleon pole is also considered as the background. Since there are large uncertainties for the mass and width of the $\Lambda(1600)$ resonance, we will vary them to reproduce the experimental data. While for the
$\Lambda(1670)$ resonance, we take the average values for its mass and width as quoted in the Particle Data Group (PDG) [29]. The total and differential cross sections of the $K^-p \to \Lambda\pi^0\pi^0$ reaction are calculated. It is found that the contribution of the $\Lambda(1600)$ resonance is significant, and the experimental data on the total cross sections and angular distributions, around the reaction energy region of the $\Lambda(1600)$ state, can be well reproduced with the model parameters.

The present paper is organized as follows: In section 2, we discuss the formalism and the main ingredients for our theoretical calculations; In section 3 we present our numerical results and conclusions; A short summary is given in the last section.

2. Formalism and ingredients

The combination of the resonance model and the effective Lagrangian approach is an important theoretical tool in describing the various scattering processes in the resonance production region [30–33]. In this section, we introduce the theoretical formalism and ingredients to study the $K^-p \to \Lambda\pi^0\pi^0$ reaction by using the effective Lagrangian approach and resonance model.

2.1. Feynman diagrams and effective interaction Lagrangian densities

The basic tree-level Feynman diagrams for the $K^-p \to \Lambda\pi^0\pi^0$ reaction are shown in figure 1. These include s-channel Λ^* resonances process (figure 1(a)) and u-channel nucleon pole diagram (figure 1(b)). For the $\pi^0\Lambda$ production, we consider only the contribution from $\Sigma^*(1385)$. The t-channel K^+ exchange term via $K^+K^- \to \pi^0\pi^0$ transition is not considered since its contribution is rather small. Additionally, the t-channel K^* exchange is also neglected since this mechanism is very suppressed due to the highly off-shell effect of the K^* propagator when the $\pi^0\Lambda$ invariant mass is close to the $\Sigma^*(1385)$ mass.

To evaluate the contributions of those terms shown in figure 1, the effective Lagrangian densities for relevant interaction vertexes are needed. Following [34–40], the Lagrangian densities used in this work are,

$$\mathcal{L}_{\Lambda_1^*\bar{K}N} = -\frac{g_{\Lambda_1^*\bar{K}N}}{m_N + M_{\Lambda_1^*}}\bar{\Lambda}_1^*\gamma_5\gamma_\mu\partial^\mu\phi_{\bar{K}}N + \text{h.c.}, \tag{3}$$

$$\mathcal{L}_{\Lambda_1^*\pi\Sigma^*} = \frac{g_{\Lambda_1^*\pi\Sigma^*}}{m_\pi}\bar{\Sigma}_\mu^*\partial^\mu(\vec{\tau}\cdot\vec{\pi})\Lambda_1^* + \text{h.c.}, \tag{4}$$

Table 1. Relevant parameters used in the present calculation. The masses, widths and branching ratios of $\Lambda(1670)$ and $\Sigma^*(1385)$ resonances are taken from PDG [29], while for the $\Lambda(1600)$ resonance, these values are determined to the experimental data.

State (J^P)	Mass (MeV)	Width (MeV)	Decay mode	Branching ratio (%)	$g^2/4\pi$
$\Sigma^*(1385)$ $(\frac{3}{2}^+)$	1385	37	$\pi\ \Lambda$	87	0.12
$\Lambda(1670)$ $(\frac{1}{2}^-)$	1670	35	$\bar{K}N$	25	0.009
			$\pi\Sigma^*(1385)$	22.4	1.07
$\Lambda(1600)$ $(\frac{1}{2}^+)$	1580	150	$\bar{K}N$	22.5	1.56
			$\pi\Sigma^*(1385)$	6.5	0.05

$$\mathcal{L}_{\Lambda_2^*\bar{K}N} = g_{\Lambda_2^*\bar{K}N}\bar{\Lambda}_2^*\phi_{\bar{K}}N + \text{h.c.}, \tag{5}$$

$$\mathcal{L}_{\Lambda_2^*\pi\Sigma^*} = \frac{g_{\Lambda_2^*\pi\Sigma^*}}{m_\pi}\bar{\Sigma}_\mu^*\gamma_5\partial^\mu(\vec{\tau}\cdot\vec{\pi})\Lambda_2^* + \text{h.c.}, \tag{6}$$

$$\mathcal{L}_{\pi\Lambda\Sigma^*} = \frac{g_{\pi\Lambda\Sigma^*}}{m_\pi}\bar{\Sigma}_\mu^*\partial^\mu(\vec{\tau}\cdot\vec{\pi})\Lambda + \text{h.c.}, \tag{7}$$

$$\mathcal{L}_{\bar{K}N\Sigma^*} = \frac{g_{\bar{K}N\Sigma^*}}{m_{\bar{K}}}\bar{\Sigma}_\mu^*\partial^\mu\phi_{\bar{K}}N + \text{h.c.}, \tag{8}$$

$$\mathcal{L}_{\pi NN} = -\frac{g_{\pi NN}}{2m_N}\bar{N}\gamma_5\gamma_\mu\partial^\mu(\vec{\tau}\cdot\vec{\pi})N, \tag{9}$$

where Σ_μ^* is the Rarita-Schwinger field of the $\Sigma^*(1385)$ resonance with spin $\frac{3}{2}$, and $\vec{\tau}$ is a usual isospin-1/2 Pauli matrix operator.

For the coupling constants in the above Lagrangian densities for the u-channel process, we take $g_{\pi NN} = 13.45$ and $g_{N\bar{K}\Sigma^*} = -3.19$ which are used in previous works [41–43] for studying different processes. For the coupling constant $g_{\pi\Lambda\Sigma^*(1385)}$ and $g_{\Lambda(1670)\bar{K}N}$, they can be determined from the experimental observed partial decay widths of $\Sigma^*(1385) \to \pi\Lambda$ and $\Lambda(1670) \to \bar{K}N$, respectively.

With the effective interaction Lagrangians described by equations (3), (5), and (7), the partial decay widths $\Gamma_{\Sigma^*\to\pi\Lambda}$ and $\Gamma_{\Lambda_2^*\to\bar{K}N}$ can be easily obtained [29]. The coupling constants related to the partial decay widths are written as,

$$\Gamma_{\Lambda_1^*\to\bar{K}N} = \frac{g^2_{\Lambda_1^*\bar{K}N}}{2\pi}(E_N - m_N)\frac{p_{\bar{K}N}}{M_{\Lambda_1^*}}, \tag{10}$$

$$\Gamma_{\Lambda_2^*\to\bar{K}N} = \frac{g^2_{\Lambda_2^*\bar{K}N}}{2\pi}(E_N + m_N)\frac{p_{\bar{K}N}}{M_{\Lambda_2^*}}, \tag{11}$$

$$\Gamma_{\Sigma^*\to\pi\Lambda} = \frac{g^2_{\Sigma^*\pi\Lambda}}{12\pi}(E_\Lambda + m_\Lambda)\frac{p^3_{\pi\Lambda}}{m_\pi^2 m_{\Sigma^*}}, \tag{12}$$

with

$$E_N = \frac{M^2_{\Lambda_1^*/\Lambda_2^*} + m_N^2 - m_{\bar{K}}^2}{2M_{\Lambda_1^*/\Lambda_2^*}}, \tag{13}$$

$$p_{\bar{K}N} = \sqrt{E_N^2 - m_N^2}, \tag{14}$$

$$E_\Lambda = \frac{m^2_{\Sigma^*} + m_\Lambda^2 - m_\pi^2}{2m_{\Sigma^*}}, \tag{15}$$

$$p_{\pi\Lambda} = \sqrt{E_\Lambda^2 - m_\Lambda^2}. \tag{16}$$

With the masses, widths and branching ratios of $\Lambda(1670)$ and $\Sigma^*(1385)$ resonances quoting in PDG [29], the numerical results for the relevant coupling constants are listed in table 1, while the other coupling constants needed in this work will be discussed below.

2.2. Propagators and form factors

To get the scattering amplitude of the $K^-p \to \Lambda\pi^0\pi^0$ reaction corresponding to the Feynman diagrams shown in figure 1, we also need the propagators for spin $\frac{1}{2}$ particles: nucleon, $\Lambda(1600)$ and $\Lambda(1670)$, and $\Sigma^*(1385)$ resonance with spin $\frac{3}{2}$,

$$G_p(q_u) = \mathrm{i}\frac{\not{q}_u + m_N}{q_u^2 - m_p^2}, \tag{17}$$

$$G_{\Lambda_1^*/\Lambda_2^*}(q_s) = \mathrm{i}\frac{\not{q}_s + M_{\Lambda_1^*/\Lambda_2^*}}{q_s^2 - M^2_{\Lambda_1^*/\Lambda_2^*} + \mathrm{i}M_{\Lambda_1^*/\Lambda_2^*}\Gamma_{\Lambda_1^*/\Lambda_2^*}}, \tag{18}$$

$$G^{\mu\nu}_{\Sigma^*}(q_{\Sigma^*}) = \mathrm{i}\frac{(\not{q}_{\Sigma^*} + m_{\Sigma^*})P^{\mu\nu}(q_{\Sigma^*})}{q^2_{\Sigma^*} - m^2_{\Sigma^*} + im_{\Sigma^*}\Gamma_{\Sigma^*}}, \tag{19}$$

with

$$P^{\mu\nu}(q_{\Sigma^*}) = -g^{\mu\nu} + \frac{1}{3}\gamma^\mu\gamma^\nu + \frac{2}{3}\frac{q^\mu_{\Sigma^*}q^\nu_{\Sigma^*}}{m^2_{\Sigma^*}} + \frac{1}{3m_{\Sigma^*}}(\gamma^\mu q^\nu_{\Sigma^*} - \gamma^\nu q^\mu_{\Sigma^*}), \tag{20}$$

where q_u, q_s and q_{Σ^*} are the momenta of nucleon pole in u-channel, $\Lambda(1600)$ or $\Lambda(1670)$ resonance in s-channel, and $\Sigma^*(1385)$ resonance, respectively.

Finally, we also need to include the off-shell form factors in the scattering amplitudes. There is no unique theoretical way to introduce the form factors, hence, we adopt here the common scheme used in many previous works [42–44],

$$f_i = \frac{\Lambda_i^4}{\Lambda_i^4 + (q_i^2 - M_i^2)^2}, \quad i = s, u, \Sigma^* \tag{21}$$

$$\text{with} \quad \begin{cases} q_s^2 = s, q_u^2 = u, q^2_{\Sigma^*} = M^2_{\pi^0\Lambda} \\ M_u = m_N, M_{\Sigma^*} = m_{\Sigma^*}, \\ M_s = M_{\Lambda_1^*/\Lambda_2^*}, \end{cases} \tag{22}$$

where s and u are the Lorentz-invariant Mandelstam variables, while $M_{\pi^0\Lambda}$ is the invariant mass of the $\pi^0\Lambda$ system. In the present calculation, $q_s = p_1 + p_2$, $q_u = p_2 - p_3$, and $q_{\Sigma^*} = p_4 + p_5$ are the 4-momenta of intermediate $\Lambda(1600)$ or

$\Lambda(1670)$ resonance, exchanged nucleon pole in the u-channel, and the $\Sigma^*(1385)$ resonance decaying into $\pi^0\Lambda$, respectively, while p_1, p_2, p_3, p_4, and p_5 are the 4-momenta for K^-, p, π^0, π^0, and Λ, respectively. Additionally, we will consider the same cut-off values for the background and resonant terms, i.e. $\Lambda_s = \Lambda_u$. Note that the numerical results are not sensitive to Λ_s and Λ_{Σ^*}.

2.3. Scattering amplitudes

With the effective interaction Lagrangian densities given above, we can easily construct the invariant scattering amplitudes for the $K^-p \to \Lambda\pi^0\pi^0$ reaction corresponding to the diagrams shown in figure 1:

$$\mathcal{M} = \mathcal{M}(\Lambda_1^*) + \mathcal{M}(\Lambda_2^*) + \mathcal{M}(N). \tag{23}$$

Each of the above amplitudes can be obtained straightforwardly as,

$$\mathcal{M}(i) = \bar{u}(p_5, s_\Lambda) G^{\mu\nu}_{\Sigma^*} \mathcal{A}_{\mu\nu}(i) u(p_2, s_p), \tag{24}$$

where s_Λ and s_p are the spin polarization variables for the final Λ and initial proton, respectively. The reduced $A^{\mu\nu}(i)$ can also be easily obtained:

$$\mathcal{A}^{\mu\nu}(\Lambda_1^*) = -\mathrm{i} g_1 p_4^\mu p_3^\nu G_{\Lambda_1^*}(q_s)\gamma_5 \not{p}_1 f_s(\Lambda_1^*) f_{\Sigma^*}, \tag{25}$$

$$\mathcal{A}^{\mu\nu}(\Lambda_2^*) = g_2 p_4^\mu p_3^\nu \gamma_5 G_{\Lambda_2^*}(q_s) f_s(\Lambda_2^*) f_{\Sigma^*}, \tag{26}$$

$$\mathcal{A}^{\mu\nu}(N) = -\mathrm{i} g_3 p_4^\mu p_1^\nu G_N(q_u)\gamma_5 \not{p}_3 f_u f_{\Sigma^*}, \tag{27}$$

with

$$g_1 = \frac{g_{\Sigma^*\pi\Lambda} g_{\Lambda_1^*\pi\Sigma^*} g_{\Lambda_1^* \bar{K} N}}{m_\pi^2 (m_N + M_{\Lambda_1^*})}, \tag{28}$$

$$g_2 = \frac{g_{\Sigma^*\pi\Lambda} g_{\Lambda_2^*\pi\Sigma^*} g_{\Lambda_2^* \bar{K} N}}{m_\pi^2}, \tag{29}$$

$$g_3 = \frac{g_{\Sigma^*\pi\Lambda} g_{\Sigma^*\bar{K}N} g_{\pi NN}}{2 m_\pi m_{\bar{K}} m_N}. \tag{30}$$

Then, the cross section for the $K^-p \to \Lambda\pi^0\pi^0$ reaction can be calculated by [29, 45] [4]

$$\mathrm{d}\sigma = \frac{1}{4}\frac{1}{(2\pi)^5} \frac{m_p}{\sqrt{(p_1\cdot p_2)^2 - m_p^2 m_{K^-}^2}} \times \sum_{s_p, s_\Lambda} |\mathcal{M}|^2 \times \frac{\mathrm{d}^3 p_3}{2E_3}\frac{\mathrm{d}^3 p_4}{2E_4}\frac{m_\Lambda \mathrm{d}^3 p_5}{E_5}\delta^4(p_1 + p_2 - p_3 - p_4 - p_5) \tag{31}$$

$$= \frac{1}{2^{10}\pi^5} \frac{m_p m_\Lambda}{\sqrt{s[(p_1\cdot p_2)^2 - m_p^2 m_{K^-}^2]}} \sum_{s_p, s_\Lambda} |\mathcal{M}|^2 \tag{32}$$

$$\times |\vec{p}_3||\vec{p}_5{}^*| \mathrm{d}M_{\pi^0\Lambda} \mathrm{d}\Omega_3 \mathrm{d}\Omega_5^*, \tag{33}$$

with $s = (p_1 + p_2)^2 = m_p^2 + m_{K^-}^2 + 2p_1\cdot p_2$, and $\vec{p}_5{}^*$ and Ω_5^* are the three-momentum and solid angle of the out going Λ in the c.m. frame of the final $\pi^0\Lambda$ system, while $\vec{p}_3$ and Ω_3 are the three-momentum and solid angle of the π^0 meson in the c.m. frame of the initial K^-p system. Note that we have already taken into account the factor $1/2$ for the identity of the two pions in the final state.

[4] Note that the total squared amplitude for $K^-p \to \pi^0\pi^0\Lambda$ reaction is symmetrized in the momenta p_3 and p_4 to account for the two π^0 in the final state.

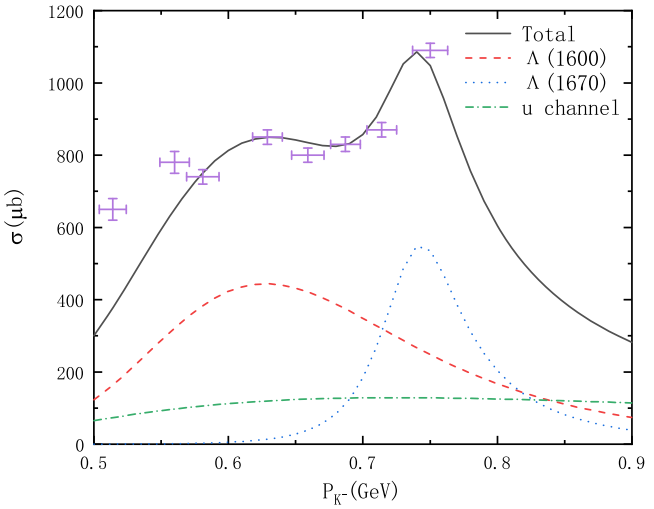

Figure 2. Theoretical results of the total cross sections of the $K^-p \to \Lambda\pi^0\pi^0$ reaction. The experimental data are taken from [22].

3. Numerical results and discussions

The theoretical results for the total cross sections for beam momenta p_{K^-} (module of the three momentum $\vec{p}_1$) from 0.5 to 0.9 GeV are shown in figure 2, where we have investigated the role of $\Lambda(1600)$, $\Lambda(1670)$ and the u-channel process in describing the total cross sections. The contributions from different mechanisms are shown separately. The red dashed, blue dotted, and green dash-dotted curves stand for contributions from the $\Lambda(1600)$, $\Lambda(1670)$ and u-channel, respectively. Their total contributions are shown by the solid line. The theoretical numerical results are obtained with the following parameters: $\Lambda_s = 600$ MeV for the $\Lambda(1600)$ and $\Lambda(1670)$ resonances, $\Lambda_u = \Lambda_{\Sigma^*} = 600$ MeV, $M_{\Lambda_1^*} = 1580$ MeV, $\Gamma_{\Lambda_1^*}$ =150 MeV, $g_{\Lambda_1^*\pi\Sigma^*} = 0.79$ and $g_{\Lambda_2^*\pi\Sigma^*} = 3.67$.

From figure 2, one can see that we can reproduce the experimental data of [22] fairly well, and that the $\Lambda(1600)$ resonance gives a dominant contribution to the reaction around $p_{K^-} = 630$ MeV, while the contribution of $\Lambda(1670)$ is significant around $p_{K^-} = 750$ MeV. On the other hand, it is seen clearly that the inclusion of the $\Lambda(1600)$ resonance is crucial to achieve a fairly good description of the experimental data. However, we can not describe the enhancement at the low energy region, where it could be explained by the tail of the contribution of the $\Lambda(1520)$ in [24, 25], and it may also be explained by the possible $\Sigma^*(1380) \to \pi\Lambda$ in the s wave as proposed in [28]. Such calculations are beyond the scope of the present investigation but we will clarify this issue in a future study.

With the obtained strong coupling constants $g_{\Lambda_1^*\pi\Sigma^*}$ and $g_{\Lambda_2^*\pi\Sigma^*}$, we have evaluated the $\Lambda(1600)$ and $\Lambda(1670)$ resonances to the $\pi\Sigma^*(1385)$ partial decay width:

$$\Gamma_{\Lambda_1^*/\Lambda_2^*\to\pi\Sigma^*} = \frac{g^2_{\Lambda_1^*/\Lambda_2^*\pi\Sigma^*} M_{\Lambda_1^*/\Lambda_2^*}}{6\pi m_\pi^2 m_{\Sigma^*}}(E_{\Sigma^*} \pm m_{\Sigma^*}) p^3_{\pi\Sigma^*},$$

with

$$E_{\Sigma^*} = \frac{M^2_{\Lambda_1^*/\Lambda_2^*} + m^2_{\Sigma^*} - m^2_\pi}{2M_{\Lambda_1^*/\Lambda_2^*}}, \tag{34}$$

$$p_{\pi\Sigma^*} = \sqrt{E^2_{\Sigma^*} - m^2_{\Sigma^*}}, \tag{35}$$

as deduced from the Lagrangians of equations (4) and (6). With the partial decay widths, we can then obtain the branching ratios. The numerical predictions for these branching ratios are also given in table 1. Note that the uncertainties of the coupling constants and cut off parameters are not studied in this work, since, including such effects, the scattering amplitudes would be more complex due to additional model parameters, and we cannot exactly determine these parameters. Thus, we leave these investigations to further studies when more precise experimental measurements become available.

In addition to the total cross sections, we also compute the angle distributions for $K^-p \to \Lambda\pi^0\pi^0$ reaction. The corresponding theoretically numerical results at $p_{K^-} = 581$, 629, and 687 MeV, where the contribution of the $\Lambda(1600)$ resonance is dominant, are shown in figure 3. For comparison, we also show the experimental data from [22]. It is obvious that we can reproduce the current experimental data on the angular distribution of the $K^-p \to \Lambda\pi^0\pi^0$ reaction fairly well, thanks to the contribution of the $\Lambda(1600)$ resonance.

Finally, in figure 4, we show the theoretical results on the differential cross section $d\sigma/dM_{\pi^0\Lambda}$ as a function of the invariant mass of a pair of $\pi^0\Lambda$ for the values of K^- momentum 581, 629 and 687 MeV. From these figures, we see that the shape of the $\pi^0\Lambda$ invariant mass distributions are different as the beam energy is increasing. We hope that the future experimental measurements can check our model calculations.

4. Summary

In summary, we have investigated the total and differential cross sections of the $K^-p \to \Lambda\pi^0\pi^0$ reaction within an effective Lagrangian approach and the resonance model. The role played by the $\Lambda(1600)$ and $\Lambda(1670)$ resonances are studied. It is shown that our model calculations lead to a fair description of the experimental data on the total cross section except for the low energy date. The scheme proposed herein should be supplemented with some other reaction mechanisms which could improve the achieved description of the low energy enhancement. Indeed, as is proposed in [24, 25] the $\Lambda(1520)$ plays an important role in the $K^-p \to \Lambda\pi^0\pi^0$ reaction with the $K^-p \to \pi\Sigma^*(1385)$ amplitude obtained from the chiral unitary approach. However, we have shown here that

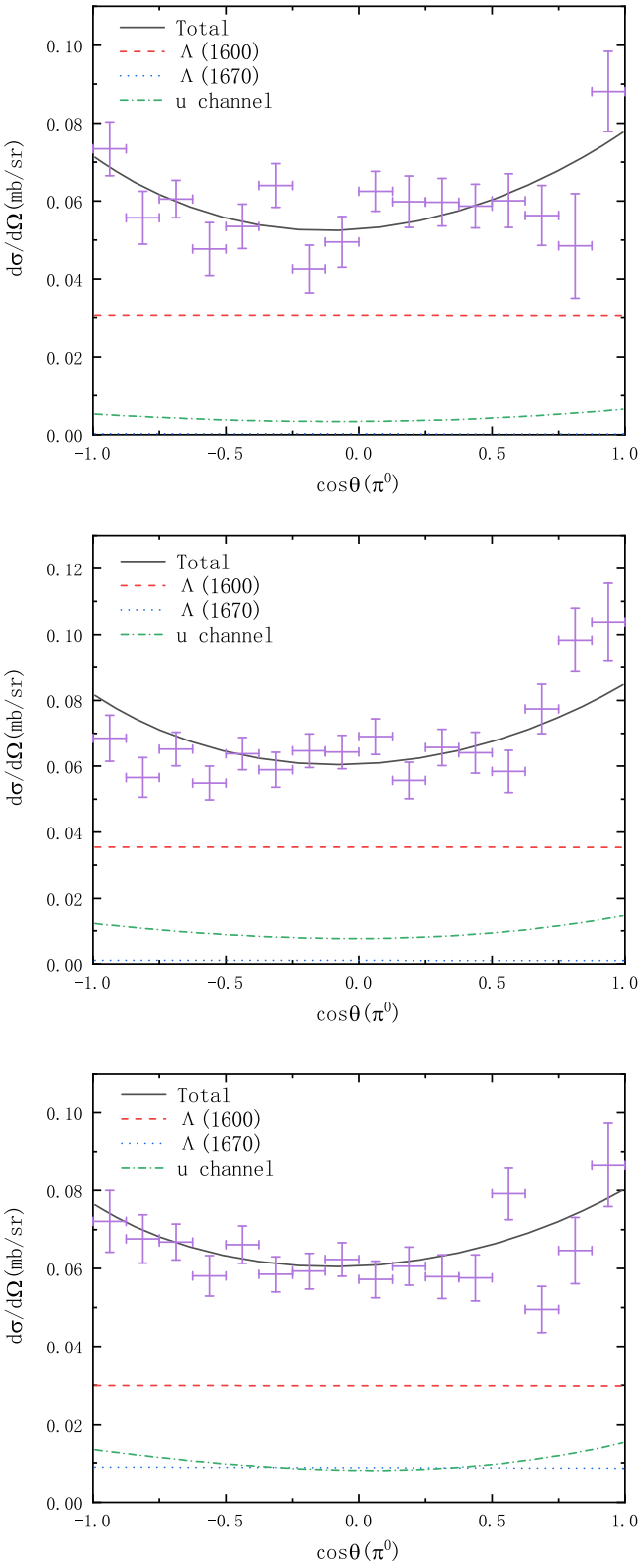

Figure 3. Angular differential cross sections for the $K^-p \to \Lambda\pi^0\pi^0$ reaction as a function of $\cos\theta$ with θ the angel between the π^0 direction and the beam direction in the overall c.m. system at $p_{K^-} = 581$ (up), 629 (middle), and 687 MeV (down). The experimental data are taken from [22].

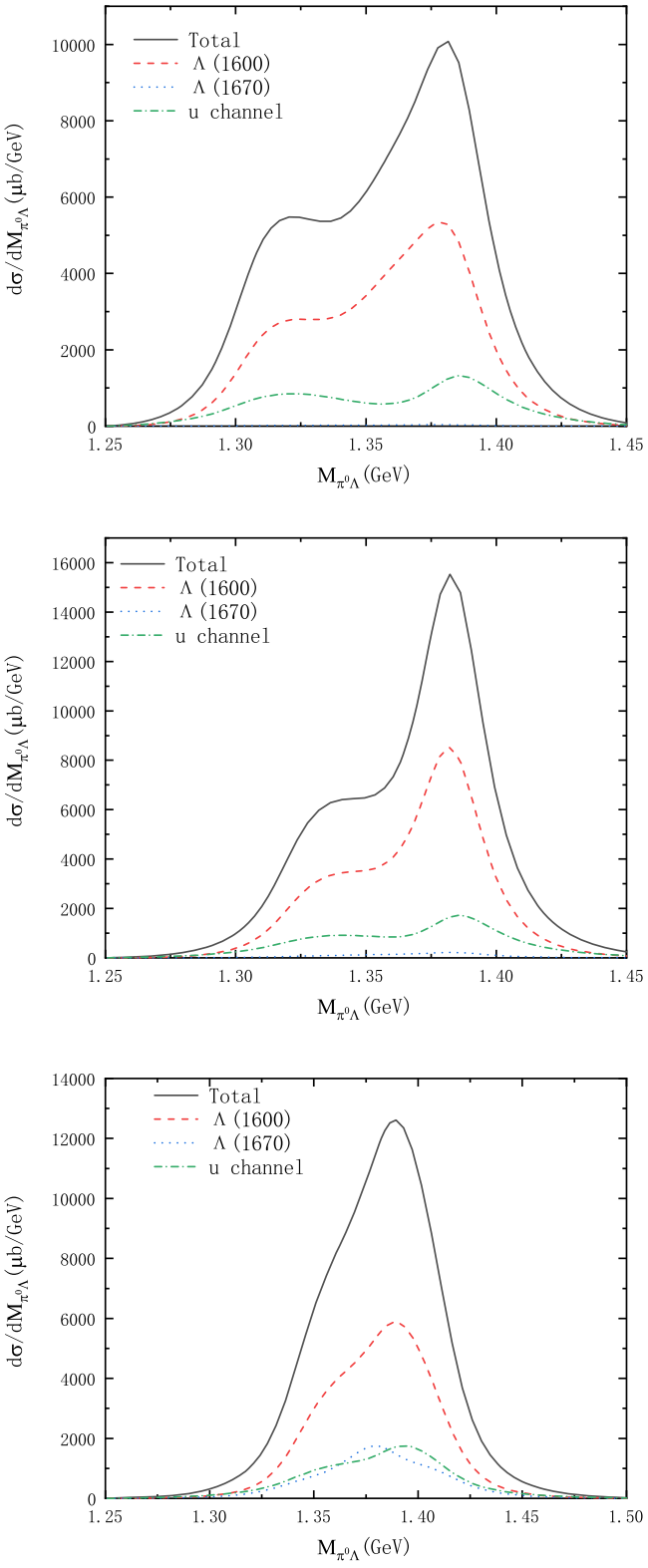

Figure 4. The $\pi^0\Lambda$ invariant mass distribution of $K^-p \to \Lambda\pi^0\pi^0$ reaction at $p_{K^-} = 581$ (up), 629 (middle), and 687 MeV (down).

the $\Lambda(1600)$ and $\Lambda(1670)$ resonances give dominant contributions, and the consideration of the $\Lambda(1600)$ resonance is crucial.

Finally, we would like to stress that, thanks to the important role played by the resonant contribution of $\Lambda(1600)$ resonance in the $K^-p \to \Lambda\pi^0\pi^0$ reaction, we can describe experimental data on the total cross section and angle distributions. Accurate data for this reaction can be used to improve our knowledge of some $\Lambda(1600)$ properties, which are at present poorly known. This work constitutes a first step in this direction.

Acknowledgments

One of us (He Zhou) would like to thank Xu Zhang for useful discussions. This work is partly supported by the National Natural Science Foundation of China under Grant Nos. 11735003, 1191101015 and 11475227, and by the Youth Innovation Promotion Association CAS (No. 2016367).

References

[1] Khemchandani K P, Martínez Torres A and Oller J A 2019 *Phys. Rev.* C **100** 015208
[2] Sadasivan D, Mai M and Döring M 2019 *Phys. Lett.* B **789** 329
[3] Feijoo A, Magas V and Ramos A 2019 *Phys. Rev.* C **99** 035211
[4] Guo Z H and Oller J A 2013 *Phys. Rev.* C **87** 035202
[5] Zhang H, Tulpan J, Shrestha M and Manley D M 2013 *Phys. Rev.* C **88** 035204
[6] Zhang H, Tulpan J, Shrestha M and Manley D M 2013 *Phys. Rev.* C **88** 035205
[7] Shi J and Zou B S 2015 *Phys. Rev.* C **91** 035202
[8] Zhong X H and Zhao Q 2009 *Phys. Rev.* C **79** 045202
[9] Prakhov S *et al* (Crystall Ball Collaboration) 2004 *Phys. Rev.* C **70** 034605
[10] Adhikari S *et al* (GlueX Collaboration) 2017 (arXiv:1707.05284 [hep-ex])
[11] Zou B S 2016 (arXiv:1603.03927 [hep-ph])
[12] Magas V K, Oset E and Ramos A 2005 *Phys. Rev. Lett.* **95** 052301
[13] Jido D, Oller J A, Oset E, Ramos A and Meissner U G 2003 *Nucl. Phys.* A **725** 181
[14] Oset E, Ramos A and Bennhold C 2002 *Phys. Lett.* B **527** 99
Oset E, Ramos A and Bennhold C 2002 *Phys. Lett.* B **530** 260 Erratum:
[15] Oset E and Ramos A 1998 *Nucl. Phys.* A **635** 99
[16] Kamano H, Nakamura S X, Lee T-S H and Sato T 2014 *Phys. Rev.* C **90** 065204
[17] Kamano H, Nakamura S X, Lee T-S H and Sato T 2015 *Phys. Rev.* C **92** 025205
Kamano H, Nakamura S X, Lee T-S H and Sato T 2017 *Phys. Rev.* C **95** 049903 Erratum:
[18] Liu B C and Xie J J 2012 *Phys. Rev.* C **85** 038201
[19] Liu B C and Xie J J 2012 *Phys. Rev.* C **86** 055202
[20] Liu B C and Xie J J 2013 *Few Body Syst.* **54** 1131
[21] Starostin A *et al* (Crystal Ball Collaboration) 2001 *Phys. Rev.* C **64** 055205
[22] Prakhov S *et al* 2004 *Phys. Rev.* C **69** 042202
[23] Xie J J, Liang W H and Oset E 2016 *Phys. Rev.* C **93** 035206
[24] Sarkar S, Oset E and Vicente Vacas M J 2005 *Phys. Rev.* C **72** 015206
[25] Roca L, Sarkar S, Magas V K and Oset E 2006 *Phys. Rev.* C **73** 045208
[26] Helminen C and Riska D O 2002 *Nucl. Phys.* A **699** 624
[27] Zhang A, Liu Y R, Huang P Z, Deng W Z, Chen X L and Zhu S L 2005 *High Energy Phys. Nucl. Phys.* **29** 250
[28] Wu J J, Dulat S and Zou B S 2010 *Phys. Rev.* C **81** 045210

[29] Tanabashi M *et al* (Particle Data Group) 2018 *Phys. Rev.* D **98** 030001
[30] Cheng C, Xie J J and Cao X 2016 *Commun. Theor. Phys.* **66** 675
[31] Wu C Z, Lü Q F, Xie J J and Chen X R 2015 *Commun. Theor. Phys.* **63** 215
[32] Xie J J and Liu B C 2013 *Phys. Rev.* C **87** 045210
[33] Xie J J, Wu J J and Zou B S 2014 *Phys. Rev.* C **90** 055204
[34] Doring M, Hanhart C, Huang F, Krewald S, Meissner U-G and Ronchen D 2011 *Nucl. Phys.* A **851** 58
[35] Xie J J, Liu B C and An C S 2013 *Phys. Rev.* C **88** 015203
[36] Xie J J, Wang E and Zou B S 2014 *Phys. Rev.* C **90** 025207
[37] Xiao L Y, Lü Q F, Xie J J and Zhong X H 2015 *Eur. Phys. J.* A **51** 130
[38] Wang A C, Wang W L and Huang F 2018 *Phys. Rev.* C **98** 045209
[39] Wang A C, Wang W L, Huang F, Haberzettl H and Nakayama K 2017 *Phys. Rev.* C **96** 035206
[40] Huang F, Haberzettl H and Nakayama K 2013 *Phys. Rev.* C **87** 054004
[41] Machleidt R, Holinde K and Elster C 1987 *Phys. Rept.* **149** 1
[42] Liu B C and Zou B S 2006 *Commun. Theor. Phys.* **46** 501
[43] Xie J J, Zou B S and Chiang H C 2008 *Phys. Rev.* C **77** 015206
[44] Xie J J and Nieves J 2010 *Phys. Rev.* C **82** 045205
[45] Xie J J, Dong Y B and Cao X 2015 *Phys. Rev.* D **92** 034029